

Proton Beam Dosimetry: a Comparison between a Plastic Scintillator, Ionization Chamber and Faraday Cup

Mitra GHERGHEREHCHI^{1,3}, Hossein AFARIDEH^{1*}, Mohammad GHANNADI³,
Ahmad MOHAMMADZADEH¹, Golam Reza ASLANI²
and Behzad BOGHRATI¹

Plastic scintillator (BC400)/Markus chamber/Faraday cap/Proton Bragg peak/CR-39.

In this study, a comparison was made between a plastic scintillator (BC400), a Faraday Cup (FC) and an ionization chamber (IC) used for routine proton dosimetry. Thin scintillators can be applied to proton dosimetry and consequently to proton therapy as relative dosimeters because of their water-equivalent nature, high energy-light conversion efficiency, low dimensions and good proportionality to the absorbed dose at low stopping powers. To employ such scintillators as relative dosimeters in proton therapy, the corrective factors must be applied to correct the quenching luminescence at the Bragg peak. A fine linear proportionality between the luminescence light yield Y and the proton flux in a thin (0.5 mm) scintillator for the 20 and 30 MeV proton beams were observed. The experimental peak/plateau ratios of Bragg Curve for 2, 1 and 0.5 mm scintillators with an accuracy of 0.5% were obtained to be 1.87, 1.91 and 2.30, respectively. With combination of the Markus chamber and the CR-39 detector, the peak/plateau ratio was improved to 3.26. The obtained data of the luminescence yield as a function of the specific energy loss is in agreement with the Craun-Birk's theory. Results show that the FC and Markus ionization chamber are in agreement within 4%, while the FC gives a lower dose evaluation. For a defined beam, the data for the fluence measurements are reproducible within a good accuracy.

INTRODUCTION

Due to the lack of national standards and absolute dosimeter in proton dosimetry, we are forced to use relative dosimeters for proton dosimetry. In this work, the possibility of using the Faraday Cup (FC) as a secondary standard dosimetry for the clinical proton dosimetry has been studied.^{1,2} Our FC optimum construction and design parameters were selected from a review done by Cambria R, *et al.*³ Moreover, a plastic scintillator detector such as polyvinyltoluene (PVT) has a high sensitivity for electrons and protons. It also permits detection of single ions^{4,5} and therefore it is suitable for relative dose measurements in proton dosimetry. The solid PVT scintillator is available in large sizes with various

thicknesses as thin as a few hundred microns. The main disadvantage of using a PVT scintillator is its quenching effect. Therefore, its correction factor has to be measured and has to be factored in to the obtained final results. To measure the proton dose delivered to the PVT scintillator medium, the light yield is first converted to readable signals through a photomultiplier, preamplifier and an amplifier.⁶

The thin PVT scintillators are quite suitable for relative proton dosimetry because of their water equivalent nature, high energy-light conversion efficiency, and good proportionality to the absorbed dose at low stopping powers. Due to its water equivalence characteristics, it allows us to insert them inside the human body to measure the relative doses and to verify treatment plans. In this study, the PVT plastic organic scintillator as a relative dosimeter in proton dosimetry will be examined, evaluated and compared with the FC and calibrated homemade ionization chamber (IC). The home made Markus Ionization Chamber was calibrated by the Secondary Standard Dosimetry Laboratory prior to the experiment and was utilized as a standard dosimeter for the purposes of measurement and comparison. It is worthwhile mentioning that the Markus Ionization Chamber is known as one of the most reliable devices for relative proton dosimetry. Furthermore, a properly designed Faraday Cup (FC) can

*Corresponding author: Phone: +98-21-66419506,
Fax: +98-21-66495519,
E-mail: hafarideh@aut.ac.ir

¹Department of Nuclear Engineering & Physics, Amirkabir University of Technology, P.O. Box 15875-4413, Tehran, Iran; ²Nuclear Medicine Research Group (NMRG), Agricultural, Medical and Industrial Research School, Karaj, Iran; ³Nuclear Science and Technology Research Institute (NSTRI), P.O. Box 14395-836, Tehran, I. R. of Iran.

doi:10.1269/jrr.09121

be used as one of the standard tools to measure the current in the accelerator and accordingly the measured current is converted to the dose.

MATERIAL AND METHODS

PVT scintillator irradiation

The plastic scintillator PVT which is produced by Bicon and is known as BC400⁷⁾ was employed in this research to detect energetic protons.

The PVT conversion efficiency of released-energy per light-yield is rather high (about 2% with 30 MeV protons). The BC400 scintillators employed were thin sheets with surface of 3*3 cm² and thickness ranging between 0.5 to 2 mm. All BC400 scintillators were polished to be highly transparent to the visible light and covered by a 100 μm Teflon film and a 100 μm aluminum foil to improve the collection of the light produced by the protons and a 100 μm black polyethylene film was used as coverage to reduce the external light infiltration. To obtain high detection efficiency, the scintillator was coupled to a high sensible photo-multiplier (Electron Tube 9143B)⁸⁾ with the “Viscasil” adhesive. The luminescence light yield and the beam charge were measured with acquisition time of 60 seconds for each measurement.

Dose calculation with faraday cup

The Faraday Cap (FC) was mounted while insulated to the end port section of the aluminum Vacuum Chamber. A Guard Ring made of copper was attached to the cup held at -300 V and insulated by a high resistivity plastic material placed inside the Vacuum Chamber with 40 cm in diameter.

The dose calculation in water is given by the relation

$$D_w = \frac{1}{A} \left(\frac{S(E)}{\rho} \right)_w \frac{Q}{e} 1.602 \times 10^{-10} \quad (\text{Gy}) \quad (1)$$

where A is the effective beam area in cm², $(S(E)/\rho)_w$ is the mean stopping power in water in MeV cm² g⁻¹ at the considered proton energy E , Q is the total charge transported by the beam in coulomb, and e is the elementary charge in coulomb. For the experimental 30 MeV proton beam the stopping power in water⁹⁾ is $S(E)/\rho$ 19.03 MeV cm² g⁻¹. The elastic nuclear interactions are also included: their ratio to the electronic stopping power is about 0.05%.⁹⁾

Ionization chamber dosimetry

The 8.6 cm³ homemade Markus type ionization chamber with an electrode spacing of 2 mm and a wall thickness of 1 mm was calibrated according to the international protocols and employed for the absolute dose and dose-rate measurements at the Secondary Standard Dosimetry Laboratory (SSDL).

The Bragg curves were measured with a Markus type Parallel Plate Ionization Chamber (PPIC) and a Solid State

Detector CR-39. The collector and guard ring made of Lucite along with the conductive coatings were held at 400 to 450 V. The collected ionization charge was measured by a commercial electrometer (PTW- UNIDOS) with a sensitivity of 10 fC. Due to the Markus Chamber wall thickness of 1 mm we were limited to see the Bragg Peak position and its falling tail. In order to resolve this problem we used the CR-39 detectors with various thicknesses. The CR-39 solid state detectors are the best and most suitable detectors for detection of charged particles and specially protons.¹⁰⁾ The CR-39 detector is highly accurate because of the high number of registered tracks in the detector and accuracy of better than 1% is easily achieved. After proton irradiation, the CR-39 detectors were etched in an optimum condition (in a solution of 6 N NaOH at 70°C over a 6-hour period) in order to observe the proton tracks registered in each detector. The etched tracks were later observed using an optical microscope. The tracks appeared as dark spots on a clear white background which provided the counting and the track diameter measurements. The microscope image was viewed with a high-quality camera, which was connected to a home developed PC-based image analyzer. The image analyzer displays images on a monitor. The proton dose and energy can be determined by counting the number of proton tracks and by measurement of their diameters, respectively.¹¹⁾

Wire scanner

To determine the beam profile an automated wire scanner system¹²⁾ was employed. The wire scanner allows very small beam sizes to be scanned and measured by the designed wire scanner. We originally designed and constructed a 20-cm cubic aluminum wire scanner box and installed it on the beam line in the R&D room at NRCAM’s Cyclotron Department to measure the proton beam profiles, as presented in Fig. 1.¹³⁾

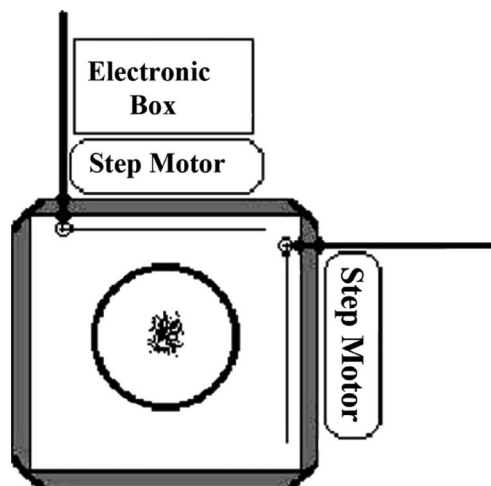


Fig. 1. Wire scanners and their mechanical assembly inside the vacuum chamber.

This profile monitor system is based on placing 2 separate isolated 0.6 mm thick and 80 mm long stainless steel wires that are mounted installed in the path of the beam for scanning it in the both x- and y-directions. By scanning the beam a signal proportional to the number of particles hitting the wire is generated from which measuring the beam profiles are made possible.

The electronic circuit is specially designed so to be able to detect the induced charges on each wire to as low as a few nano-Amps.¹³⁾

SRIM simulation

SRIM is a group of programs which calculate the stopping and range of ions (up to 2 GeV/amu) into matter using a quantum mechanical treatment of ion-atom collisions. This calculation is made very efficient by the use of statistical algorithms which allow the ion to make jumps between calculated collisions and then averaging the collision results over the intervening gap.

A full description of the calculation is found in the book “The Stopping and Range of Ions in Solids”, by J. F. Ziegler.¹⁴⁾ This book presents the accuracy of SRIM and shows various applications. Available on the SRIM website are plots showing SRIM stopping powers and all available experimental data for H and He ions into all targets. For protons in H target the deviation between SRIM simulation value and experimental data is about 2.8%.¹⁴⁾ The SRIM code is only a theoretical model which is based on a Monte Carlo simulation and not a slice by slice approach. Further, it does not take into effect the detector thickness, the ion scattering at the slice to slice interfaces and the nuclear reactions occurring along the ion path.

Experimental set-up

This experiment was performed by the IBA C-30 Cyclotron proton beam at the R& D low scattering room of NRCAM, Karaj. The proton beam energy was varied from 15 to 30 MeV. A copper collimator was placed at the end of the beam line to obtain a 20 mm beam spot diameter in air. The maximum collimated proton flux was 10^7 – 10^8 H/cm² s corresponding to a collimated current of 5–50 pA for the proton energy of 30 MeV in air. The central region of the thin scintillator was irradiated by the proton beam and the proton flux measurement before and after water equivalent absorber was performed by employing an aligned Faraday cup as illustrated in Fig. 2. The 5 cm in diameter Faraday cup used had a cylindrical current suppression, polarized to 300 V insulated and located at the end of the vacuum chamber with a thin Titanium entrance window. The Faraday cup electrical output was connected to a charge sensitive integrator (PTW - UNIDOS).

Various proton energies were delivered to the scintillators either by direct variation of cyclotron energy or by absorption of the beam by different thicknesses of “solid water”, a

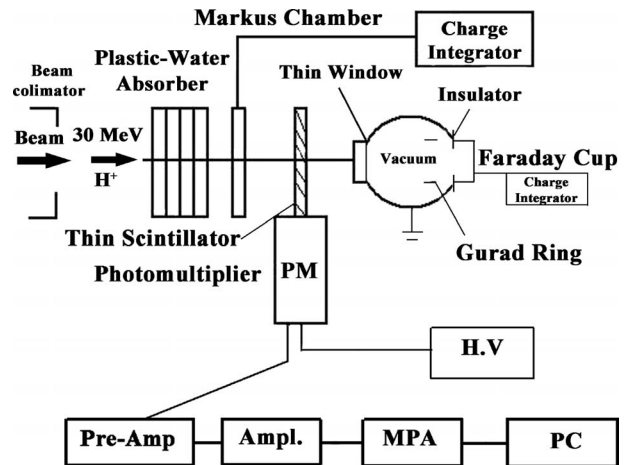


Fig. 2. The experimental setup consisting of the Faraday Cup Configuration, Scintillator Geometry, Water Absorber, Ion Chamber, and the Detection Electronics.

tissue-equivalent polymer with high water-quality characteristics¹⁵⁾ to study the scintillator responses. Scintillators with different thicknesses were placed just behind the polymer absorber (phantom) which acts as charge equilibrium medium, aligned with both surface and the beam axial direction. The absorber surface, the chamber window and the beam axial direction were all aligned. The PM-tube diameter was 1.0 inch and fed by a High Voltage Power Supply. The PMT anode output pulses were fed to the Pre-amplifier, Amplifier, and finally to the Multi Channel Analyzer. The SRIM- 2008 simulation program of Ziegler *et al*¹⁴⁾ was employed to calculate the proton stopping power.

RESULTS

A fixed guard ring voltage of -300 V³⁾ was used. No appreciable variations were seen in the range of 5×10^{-6} to 10^{-4} Torr ($\approx 0.07\%$) for the FC charge reading. However, slightly higher variations occur up to 10^{-2} Torr ($\approx 0.63\%$), while significant changes arise at higher pressure levels up to atmospheric pressure ($\approx 190\%$), where the FC behaves like an ionization chamber. Therefore, to get a good response from the FC it is not necessary to attain very low pressures ($\approx 10^{-6}$ Torr) and the pressure range of 10^{-6} to 10^{-4} Torr can be considered as a useful working range. For instance, a reachable pressure of about 10^{-4} Torr is considered to be sufficient. If the FC collection efficiency is presumed to be perfect, the main uncertainty in the fluence measurement arises from the beam area designation. The FC fluence and dose determination (Eq. 1) rely on the beam profile and the beam effective area at the measuring point. To acquire the beam profile for the 2-cm collimator, the in-house wire scanner was used to measure the beam profiles in both the x and y directions. To obtain this information, the wire

scanner must intercept the entire beam in steps of 1 mm. The data points attained were fitted to a Gaussian curve as presented in Fig. 3 and Fig. 4. The beam widths σ_x and σ_y are measured to be 5.92 and 2.25 mm, respectively. Therefore, for the 30 MeV proton beam passing through the 2 cm collimator with the triplet quadruple upstream, the effective beam area is calculated to be 42 mm². The obtained dose for the FC and the Markus chamber (IC) were 2.21 and 2.29 Gy/min, respectively.

The Bragg curve versus the target depth for a simulation of the 30 MeV proton beam incident vertically to the water target was obtained by SRIM simulation program as presented in Fig. 5.

The mean excitation energy of 74.6 eV was used for water in the above calculation. The values of 8.69 and 0.368 mm were specified for the projected range and longitudinal straggling by the simulation, respectively.

The proton stopping power at 30 MeV and at the Bragg

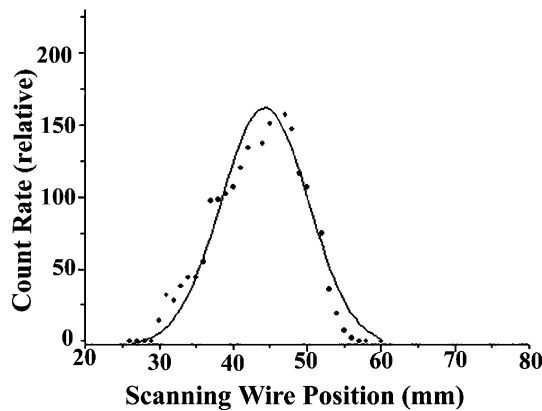


Fig. 3. Horizontal profile of the 30 MeV proton beam at the wire scanner position with $B_{T2} = 3.249$ kG. The solid line is a Gaussian fit to the data, showing $\sigma_x = 5.92$ mm.

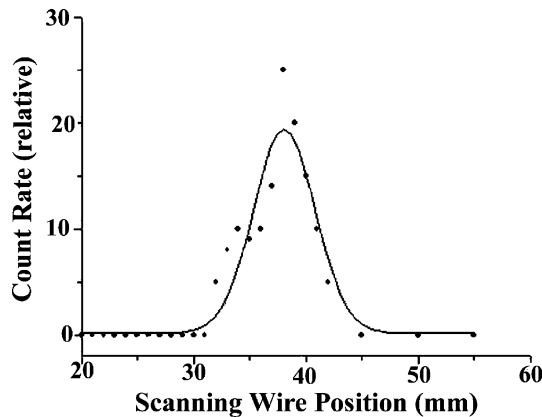


Fig. 4. Vertical profile of the 30 MeV proton beam at the wire scanner position with $B_{T2} = 3.360$ kG. The solid line is a Gaussian fit to the data, showing $\sigma_y = 2.25$ mm.

peak is 1.9 and 12.5 keV/ μ m, respectively. This corresponds to a peak/plateau ratio of 6.58. Due to ionization processes the proton energy loss is about 99.95%.¹⁴⁾

For the 20 and 30 MeV proton beams used, a fine linear proportionality is observed between the luminescence light yield Y and the proton flux in the thin (0.5 mm) scintillator as presented in Fig. 6.

The light yield is proportional to the ion energy ΔE lost in the medium for a thin scintillator with Δx thickness. The stopping power of the 30 MeV protons in PVT is about 1.96 MeV/mm and thus the energy loss in the 0.5 mm thick scintillator would be 0.98 MeV.

The recorded Bragg curves obtained by transmitting the 30 MeV proton beam through different absorber thicknesses by measuring the collected charge on the electrometers connected to the Markus, the scintillator and the Faraday cup. The results obtained for the three different scintillator thicknesses in terms of light yield per 60 s acquisition time versus absorber thickness is presented in Fig. 7.

Due to the fact that the Markus entrance window was not reasonably thin to accurately measure the Bragg peak, the

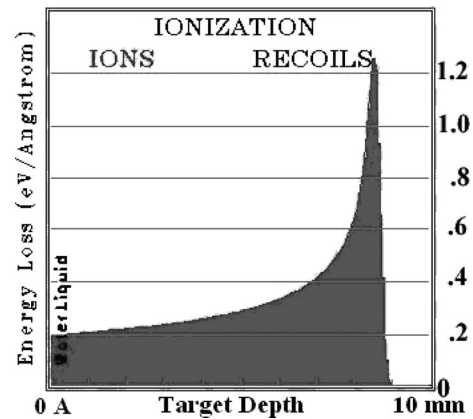


Fig. 5. Depth dose distribution of the 30 MeV proton beam.

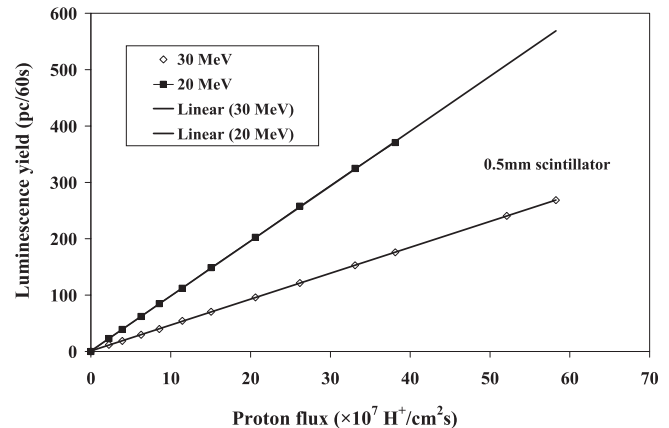


Fig. 6. Luminescence yield as a function of the particle flux for the 20 and 30 MeV proton beams.

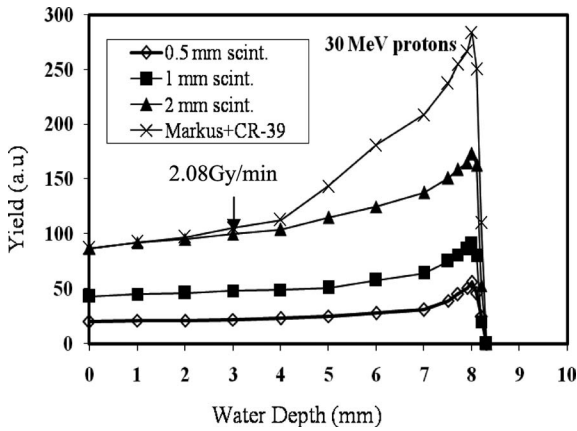


Fig. 7. Comparison of the Bragg curve obtained through using the luminescence of different thin scintillators, and the ionization of a Markus chamber or CR-39 detectors, alternatively.

CR-39 detectors were used in place of the Markus chamber.

After proton irradiation, the CR-39 detectors were etched in an optimum condition (in a solution of 6 N NaOH at 70°C over a 6-hour period) in order to observe the proton tracks registered in each detector. The etched tracks were later observed using an optical microscope. The tracks appeared as dark spots on a clear white background which provided the counting and the track diameter measurements. According to SRIM calculations the Bragg peak is located at an 8.0 mm water depth and was confirmed by our measurements. The experimental peak/plateau ratios for 2, 1 and 0.5 mm scintillators were obtained to be 1.87, 1.91 and 2.30, respectively. The accuracy of these measurements is about 0.5%. To measure the dose released in tissue as a function of depth, all the detectors alternatively were placed just behind the water-equivalent phantom by changing the absorber thickness. The Bragg curve obtained by using the luminescence of different thin scintillators when the surface signal is normalized to the 2 mm scintillator is compared with the ionization of a Markus chamber or CR-39 detectors as presented in Fig. 7. The absolute dose-rate experimentally measured by Markus for the 30 MeV proton beam given at 3 mm phantom depth, was 2.08 Gy/min (see Fig. 7). This value was used as a reference for the scintillator calibration as a relative dosimeter for the 30 MeV protons.

The peak position from the scintillator luminescence is in agreement with the Bragg peak position of the ionization curve measured with an about 0.5% accuracy but the peak/plateau ratio is significantly lower, as reported in Table 1. The scintillator luminescence yield for the 0.5 mm scintillator is obtained in terms of the light yield versus proton stopping power, and the proton stopping power values as a function of the absorber thickness were obtained by the SRIM computations as presented in Fig. 8

The obtained data shows the non-linear proportionality

Table 1. Comparison of Bragg peak/plateau ratios obtained by using different scintillators, Markus chamber and theoretical SRIM simulation.

Detector	Bragg peak position (mm)	Peak/plateau ratio
Scint. 2 mm	8.0 ± 0.15	1.99 ± 0.02
Scint. 1 mm	8.0 ± 0.15	2.14 ± 0.02
Scint. 0.5 mm	8.0 ± 0.15	2.80 ± 0.02
Markus type chamber	8.0 ± 0.15	3.26 ± 0.02
SRIM Simulation	8.2 ± 0.6	6.58

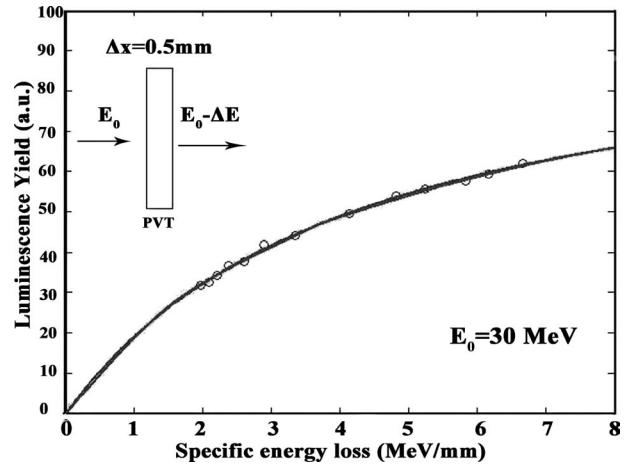


Fig. 8. Luminescence yield as a function of the specific energy loss for 0.5 mm scintillating thickness medium using 30 MeV protons.

between the collected light yield versus the energy loss ΔE per scintillator thickness Δx . This non-linear proportionality is mainly due to quenching phenomenon as the typical nature of the scintillating mediums. As shown, the luminescence yield is rather linear with the energy loss at low stopping powers while it goes toward a saturation value at high stopping powers.

Experimental data reported in Fig. 8 is in agreement with the Birk's theory for plastic scintillators. According to the following relationship¹⁶⁾:

$$dY / dx = [S / (1 + kBdE / dx)] / dE / dx \quad (2)$$

where dY/dx represents the luminescence yield per depth unit, S represents the absolute scintillator efficiency and kB represents the scintillator quenching factor. At high proton energy (low stopping powers), $kB \ll 1$ and thus,

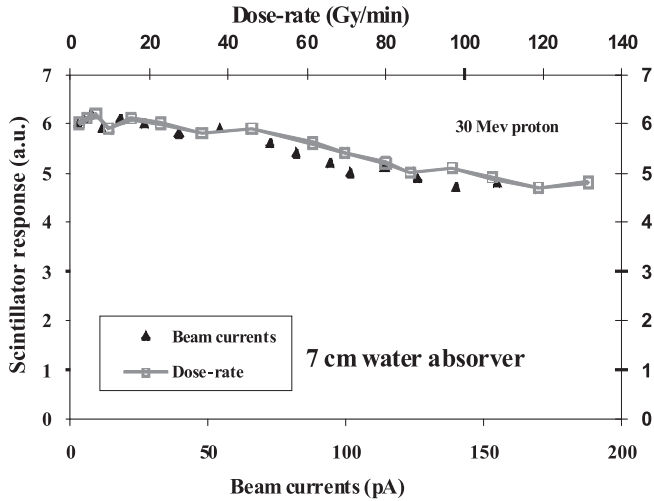
$$dY / dx \approx SdE / dx \quad (3)$$

At low proton energy (high stopping powers), $kB \gg 1$, and thus,

$$dY / dx \approx S / kB \quad \text{or} \quad Y(E) = Y_0 + (S / kB)R \quad (4)$$

Table 2. Comparison between the experimental fit data and literature.

Data	Energy (MeV)	dE/dx (MeV/mm)	KB (1° order) (g/MeV cm ²)	KB (2° order) (g/MeV cm ²)	C (g/MeV cm ²) ²	Literature
Craun and Smith	0.35–15	30–494	1.31 * 10 ⁻²	1.29 * 10 ⁻²	9.59 * 10 ⁻⁶	[17]
Gooding <i>et al.</i>	28–148	5.5–20	1.32 * 10 ⁻²			[19]
Torrissi	5–62	10–70	2.07 * 10 ⁻²	1.6 * 10 ⁻²	5 * 10 ⁻⁵	[20]
Our work	5–30	8–2	2.34 * 10 ⁻²	2.35 * 10 ⁻²	6.48 * 10 ⁻⁵	

**Fig. 9.** Independence of the scintillator light yield versus the beam current and the proton dose rate.

where Y_0 is the background light signal and R is the proton range in PVT. By fitting the data of Fig. 8 into the equation (3), the kB of about 0.2345 mm/MeV or 23.4 mg/MeV cm² was obtained which was in good agreement with the values given by Craun *et al.*¹⁷⁾ According to the second-order approximation, a better experimental data fit can be obtained through employing the Craun-Birk's theory¹⁸⁾ as given by Eq. (5).

$$dY / dx = S / [1 + kBdE / dx + C(dE / dx)^2] dE / dx \quad (5)$$

The data fitting gives $kB = 23.53$ mg/MeV cm² and $C = 6.48 * 10^{-5}$ (g/MeV cm²) which are in good agreement with the values published (Gooding *et al* and Torrissi),^{19,20)} as presented in Table 2.

The corrective factor F based on the stopping power value is used to correct the non-linearity due to the quenching effect. For instance, for the stopping power of 2.5 MeV/mm the F value is about 5% while for the 5 MeV/mm the F value increases to about 58%. In the case of thin scintillators transparent to the proton beam, having stopping powers lower than 3 MeV/mm, the non-linearity can be maintained below 10% and simultaneously the F value can be neglected. In addition, the absorbed dose measurement errors are not

acceptable for the high values of F . Therefore, it is recommended to use a very thin scintillator (0.5 mm or less) as a relative-dosimeter for the proton beam with a corrective factor of less than 10%. This low F assures an almost linear proportionality between the light yield and the absorbed dose.

Numerous measurements with the collimated 30 MeV proton beam with varying current from 2 to 100 pA have been performed and the dose-rates ranging between 3 Gy/min and 150 Gy/min for both the Markus placed behind the water absorber and the FC at the end of the beam line were obtained. During all experiments the integrated charge of protons were kept constant. As shown in Fig. 9, the results indicate almost no dependency between the dose rate and the scintillator light yield and it further shows that the measurement reproducibility occurs within 7.4%. This uncertainty is mainly due to the system beam instability and the scintillator response. At high stopping powers where significant molecular damage can occur, the radiation damage caused by protons in PVT can alter the measurement reproducibility. This molecular damage at doses of about 1 kGy seems to cause a light yield reduction of about 15%.

DISCUSSION

Our results indicate that for relative dosimeters in proton dosimetry and consequently in proton-therapy, thin plastic scintillators can be employed with caution. Although the proton energy range used in proton therapy is from 70 to 230 MeV, depending on how deep the tumor is embedded in the body, the behavior of the 30 MeV protons at the Bragg peak area is exactly similar to that of 70 to 230 MeV protons.

The light yield produced in the scintillator is proportional to the proton flux up to about 10⁸ particles/cm² s. However, due to the quenching effects at high stopping powers it loses its linearity to the absorbed dose. Moreover, for the same experimental conditions, the quenching effect would lower the luminescence yield in the Bragg peak and therefore the peak/plateau ratio becomes lower as compared with the IC and CR-39 detector measurements. As previously presented in Table 1, this ratio is somewhat dependent on the scintillator and the absorber thickness where the luminescence and the energy loss are averaged in their thickness, respectively.

The peak/plateau ratio can be enhanced by reducing the scintillators as well as the thickness of the absorber sheets. Moreover, as it is clear from Table 2, Markus chamber shows a lower peak/plateau ratio as compared to SRIM prediction.

At stopping powers higher than 3 MeV/mm where significant quenching effects occurs, the use of thin BC400 scintillator to measure modulated proton beams is not advised. In order to use such a scintillator as a relative dosimeter in proton therapy, the corrective factors must be used to correct the quenching luminescence at the Bragg peak. The average lifetime for a relative dosimeter for a very thin scintillator is very long where the released energy of the transmitted beam is minimal. For instance, a complete treatment of ocular melanoma requires 60 to 70 Gy, which is delivered in 4 to 5 steps with 12 to 15 Gy each. Therefore, a high number of treatments can be performed before reaching 1 k Gy absorbed dose at which a significant luminescence yield reduction is detectable.

The water-equivalence characteristic of the investigated scintillators allows us to insert them inside the human body to measure relative doses and to verify treatment plans.

We further conclude that it is advisable to use thin scintillators, such as 100 μm or less, to improve the Bragg peak/plateau ratio as well as the linear scintillator response with respect to the absorbed dose.

Some of the response differences between the FC and the IC are discussed below. The IC dose calculations are within 8.4% of the FC (for FC to IC ratio of 0.92) using Vynckier *et al.*¹⁾ The differences are reduced to about 5.7%, i.e. a factor 2.6% less (for FC to IC ratio of 0.95) when the AAPM protocol is used. This discrepancy is due to the different $(w_{\text{air}}/e)_p$ values prescribed by the two protocols. A detailed assessment of $(w_{\text{air}}/e)_p$ values are found in Dan's²¹⁾ article.

There are several factors that constitute the total uncertainty in the measured dose by the FC. By defining an effective value calculated from the profile and fluence measurement, the relative uncertainty on the beam area is minimized and estimated to be about 0.5%. The uncertainty on the proton energy is estimated to be about 2%. The quoted uncertainty based on the research done by Delacroix and Bridier is reported to be about 1%.²²⁾

The charge measurement uncertainty came out to be about 0.2%. All the aforementioned factors of beam area, beam energy and charge measurements constitute the total uncertainty of 2.3% on the FC dose evaluation. However, the fluence measurements uncertainty with the FC is estimated to be less than 1%.

Due to the lack of national standards for proton dosimetry and difficulty of construction and calibration of a calorimeter, therefore the FC remains as the easiest to construct and to use as an in-house fluence calibration system. The European protocol¹⁾ has recommended the IC as a secondary standard dosimeter, even if it is calibrated with a ⁶⁰Co

source. Our results show that for well defined beam characteristics the dose measurement by FC is reproducible.

ACKNOWLEDGMENTS

We are grateful to the Cyclotron Accelerator Scientific staff: Dr. Aboudzadeh, Ms. Belori, Ms. M. Jafari and the Technical staff: Mr. Ensaf and Mr. Shadanpoor for their assistance in providing the proton beam and the set up of the experimental apparatus. We further appreciate the cooperation of Mr. Arbabi and Mr. Shahvar from SSLD laboratory of NRCAM in assembling and calibration of the Markus Chamber (IC).

REFERENCES

1. Vynckier S, Bonnet DE and Jones DTL (1994) Supplement to the code of practice for clinical proton dosimetry. *Radiother Oncol* **32**: 174–179.
2. AAPM Report 16 (1989) Protocol for heavy charged-particle therapy beam dosimetry. AAPM (New York: AAPM).
3. Cambria R, *et al* (1997) Proton beam dosimetry: A comparison between the Faraday cup and an ionization chamber. *Phys Med Biol* **42**: 1185–1196.
4. Smith DL, Polk RG and Miller TG (1968) Measurement of the response of several organic scintillators to electrons, protons and deuterons. *Nucl Instrum Methods Phys* **64**: 157–166.
5. Perera H, *et al* (1992) Rapid Two-dimensional Dose Measurement in Brachytherapy Using Plastic Scintillator Sheet: Linearity, Signal-to-Noise Ratio, and Energy Response Characteristics. *Int J Radiat Oncol Biol Phys* **23**: 1059–1069.
6. Torrisi L, *et al* (1997) Bragg - Curve measurements for 24 MeV protons irradiating plastic - water. *Phys Medica* **XIII**: 117–122.
7. Bicon, (1993) Bicon catalogue: scintillation products, Newbury, USA.
8. Electron tubes limited (2001) Metal package photomultiplier tubes 9143B series, Technical information, UK, see also www.electrontubes.com.
9. ICRU (1989) Tissue substitutes in radiation dosimetry and measurements. International Communication on Radiological protection, ICRP Publication 44. Units and Meas. Maryland.
10. Durrani SA and Bull RK (1987) Solid state nuclear track detection. Pergamon Press, Oxford, UK.
11. Ghergherehchi M, *et al* (2008) Proton Beam Dosimetry by CR-39 Track-Etched Detector. *Iran J Radiat Res* **6** (3).
12. Ghergherehchi M, *et al* (2008) Extraction of 250 MeV Proton Beam by Injection of the 30 MeV Cyclotron Proton Beam into the Conceptually Designed Medical Proton Synchrotron. *IRAN J SCI TECHNOL Transaction A Vol.* **32**: No. A4, 2008.
13. Mohammadzadeh M, *et al* (2002) Beam emittance measurements in improving the energy resolution using an achromatic/dispersive system. *Radiat Meas* **35**: 229–234.
14. Ziegler JF, Biersack P and Littmark U (1986) in: J.F. Ziegler (Ed.). *The Stopping and Range of Ions in Matter*, Pergamon, New York, (new edition in 2009). See also www.SRIM.org.
15. ICRU (1993) Stopping powers and ranges for protons and

- alpha particles. International Communication on Radiological protection, ICRP Publication 49, Units and Meas. Washington.
16. Knoll GF (1989) Radiation Detection and Measurements. New York: Wiley, pp. 455.
 17. Craun RL and Smith DL (1970) Analysis of response data for several organic scintillators. Nucl Instrum Methods Phys **80**: 239–244.
 18. Birks JB (1964) Theory and Practice of Scintillation Counting. Pergamon, New York, pp. 370.
 19. Gooding TJ and Pugh HG (1960) The response of plastic scintillators to high-energy particles. Nucl Instrum Methods Phys **160**: 189–192.
 20. Torrisi L (2000) Plastic scintillator investigations for relative dosimetry in proton-therapy. Nucl Instrum Methods Phys Res SectB **170**: 523–530.
 21. Jones DTL (2006) The w-value in air for proton therapy beams. Radiat Phys Chem **75**: 541–550.
 22. Delacroix S, *et al* (1997) Proton dosimetry comparison involving ionometry and calorimetry. Int J Radiat Oncol Biol Phys **37**: 711–718.

Received on October 13, 2009

Revision received on February 3, 2010

Accepted on March 16, 2010